One step hydrothermal synthesis of $LaFeO_3$ perovskite

Jairo. A. Gómez-Cuaspud[1], Enrique. Vera-López[1], Ester Barrachina[2] and Juan. B. Carda-Castelló[2]

[1]*Universidad Pedagógica y Tecnológica de Colombia. Instituto para la Investigación e Innovación en Ciencia y Tecnología de Materiales (INCITEMA). Grupo de Integridad y Evaluación de Materiales (GIEM). Av. Central del Norte 39-115, Tunja. Colombia.*

[2] *Química del Estado Sólido, Dpto. Química Inorgánica y Orgánica, Universitat Jaume I, Castellón (España)*

E-mail: jairo.gomez01@uptc.edu.co

Corresponding author: *J. A. Gómez-Cuaspud. Universidad Pedagógica y Tecnológica de Colombia. Instituto para la Investigación e Innovación en Ciencia y Tecnología de Materiales (INCITEMA). Grupo de Integridad y Evaluación de Materiales (GIEM). Av. Central del Norte 39-115, Tunja. Colombia.*

Tel: (57+8) 7405626

E-mail address: jairo.gomez01@uptc.edu.co

Abstract

This work describes the synthesis of $LaFeO_3$ oxide, using a one-step hydrothermal synthesis route, to obtain a solid exhibiting superficial, morphological and textural properties useful for potential applications. The synthesis process starts from corresponding metal nitrates of lanthanum and iron in well-defined concentration and KOH as mineralizing agent. The reaction is developed in a Teflon-lined stainless steel autoclave at 300 °C for 14 days. The composition and surface area were determined with X-ray fluorescence (XRF) and nitrogen adsorption isotherms (BET), verifying the obtaining of a stoichiometric, high, and active phase of oxide. The crystalline structure was evaluated with X-ray diffraction analysis (XRD), showing a pure orthorhombic perovskite phase. TPR results show the development of three single steps at different temperatures, kinetically detectable and related with reduction of component oxides. Scanning and transmission electron microscopy (SEM-TEM) results showed a remarkable degree of crystallization, favouring a specific morphology as a result of the low consolidation temperature of the perovskite phase. Catalytic test by means of methane reaction, performed along 240 on stream, reveals a light deactivation rate, decreasing progressively 7.1% until 60% of methane conversion, indicating the improved morphological and surface characteristics for potential applications.

Keywords: Hydrothermal, Perovskite, Orthoferrite, Synthesis, catalytic

1. Introduction

The obtaining of advanced crystalline materials by means of the implementation of wet chemical routes has allowed the development of textural, morphological and surface properties of relevance in many fields of solid-state sciences for several nanometric applications. Particularly, in the field of synthesis of functional materials related to the use of ferrites in advanced technologies, mostly their properties have been enhanced through the implementation of synthesis routes that allow the topotactic control over compositions in aqueous medium for the consolidation of new properties. In this sense, the methods related to hydrothermal reactions, have consolidated high purity and homogeneity of final product, with low or even no reaction gas emissions (NOx, COx, SOx). This fact represents an incomparable advantage regarding other methods of synthesis, together with the possibility of obtaining metal-organic precursors with C-type surfaces and hydroxylated derivatives OH -OH, which favours their functional modification, due to the ease of implementing subsequent steps of removal of volatile species by thermal effect or dissolution in aqueous media. In this frame, Zhou *et al.*, reports that some orthoferrites obtained by implementation of these chemical routes, represent the main route for obtaining a number of ferromagnetic properties with antisymmetric interactions and certain levels of anisotropy. These properties generated by the competition between atoms Fe-Fe, Fe and La-La-La, create significant interactions, that distort the orthorhombic structure, causing significant magnetic and electrical changes for potential technological applications [P.E.

Tomaszewski, Phase Trans. 86 (2013) 260–266 **y** P.E. Tomaszewski, Wiadomosci Chem. 67 (2013) 929–942].

Therefore, present work has been limited to the synthesis and characterization of a $LaFeO_3$ perovskite by a hydrothermal synthesis route in a single step, which allowed obtaining a solid with specific textural, morphological and surface characteristics, useful for specific potential applications.

2. Experimental

2.1 Preparation of perovskite

The active phase of $LaFeO_3$ oxide was prepared by one step hydrothermal method, starting from corresponding dissolution nitrates of $La(NO_3)_3{\cdot}6H_2O$ (99.9%) and $Fe(NO_3)_3{\cdot}9H_2O$ 99.99% in a 1.0 mol L^{-1} concentration. Stoichiometric quantities of each nitrate were added in a Teflon lined steel vessel, in which a 16.0 mol L^{-1} KOH dissolution providing the alkaline medium synthesis [18]. The hydrothermal reaction was performed during 14 days at 280 °C, obtaining at the end of the process a crystalline black solid material, which was washed 6 times using absolute ethanol. Then, the solid was recovered by filtration and dried at 100 °C for its corresponding characterization. The stoichiometric composition was calculated from the global reaction, accepting the formation of

intermediate hydroxylated species which evolves as a temperature function until the consolidation of the perovskite oxide as follows:

$$La(NO_3)_3 + Fe(NO_3)_3 + KOH \rightarrow La(OH)_3 + Fe(OH)_3 \rightarrow LaFeO_3 \quad (1)$$

La reacción no está bien ajustada no?

2.2 Characterization of oxide

The chemical composition was determined using X-ray fluorescence (XRF) technique, using a Philips MagiX Pro equipment. Approximately 1.0 g of sample was treated at 400 °C for 2 hours under helium flow (5 mL min^{-1}), to remove the remaining humidity and pressed at 1.0 Mpa to form a pellet of 10 mm for quantitative analysis. The specific area BET was evaluated by nitrogen adsorption isotherms at -196 ºC, using the ASAP-2020 apparatus (Micromeritics), degassing at 350 ºC overnight under a stream of helium gas, verifying the obtaining of a high active phase of 67 m^2 g^{-1} in contrast to the same material obtained by solid-state reaction [**REFERENCE**].

The crystalline structure was determined by X-ray diffraction (XRD), in a PANalytical X'Pert PRO MPD equipment, using Cu K_α radiation (λ = 1.54186 Å) between 10° and 90°, with steps of 0.05° and a speed analysis of 0.15° min^{-1}. Refinement, indexing and the simulation of the structure was done with Rietveld method and GSAS software respectively, which allowed to evaluate the chemical composition and crystallographic structure of the perovskite. The crystallite size was calculated using the highest diffraction

signals and the Debye-Scherrer equation, taking the value of half peak width set by a Lorentzian function and using a constant of 0.89 as reference.

Temperature programmed reduction (TPR-H_2) was performed in a Chembet 300 (Quantachrome) equipment. The sample was preheated at 200 ºC for 2 h, flowing pure helium and then reduced with a mixture of 5% H_2/He (40 mL min^{-1}), rising up to the maximum temperature reduction at 10 ºC min^{-1}. The H_2 consumption was measured using a thermal conductivity detector coupled to Chembet 300 system.

Scanning and transmission electron microscopy analysis (SEM-TEM), were performed on a LEO 440 microscope (Leica-Zeis), equipped with an electron gun, while studies of transmission electron microscopy analysis (TEM) were performed on a JEOL 2100 equipment using a LaB_6 thermionic gun operated with an acceleration voltage of 200 kV, equipped with a CCD imaging system. For SEM analysis, the sample was analysed without any preparation of the same. For TEM analysis the sample was grounded and sieved at 400 U.S. standard mesh. After that, it was dispersed in a test tube with 5.0 mL of water and placed in an ultrasonic equipment for a period of 30 min, after which a drop of the top of the tube was taken and dried at 50 °C for respective analysis.

2.3 Catalytic test

The perovskite oxide was tested in the steam methane reforming reaction, which was performed in an experimental unit consisting of a set of mass flowmeters (MKS) and a reactor coupled to a resistive furnace. The reaction feed rate mixture ($CH_4/H_2O/Ar$), was 8/24/68 mL min^{-1}, respectively, pre-heated at 200ºC before catalyst contact in a U shape quartz micro-reactor with 12 mm ID and 250 mm long at 700 °C. The sample was supported on quartz wool to prevent the dispersion thereof by the feed system.

The sample was dried at 300 °C for 30 min prior catalytic tests under helium flow (30 mL min^{-1}). After cleaning and cooling, the gas valve was switched to the gas mixture and adjusted until stabilization: a GSHV = 18000 h^{-1} and a contact time of 0.20 seconds was used in all tests. The reaction was studied under isothermal conditions at 700 °C and exhaust gases were determined by gas chromatography (HP 5890 series II) equipped with a packed column HAYESEP Q of 5.5 m long, ¼" pore diameter and an inner diameter of 80/100 and a TCD detector. The FID flame detector allowed evaluating the formation of minor species.

Main products coming from methane reaction were hydrogen, methane, carbon dioxide, carbon monoxide, ethylene, ethane, acetaldehyde and diethyl ether in different proportions. The conversion of methane was calculated from carbon products in a molar balance (on dry basis), as presented in Eq. 2, where γ_{Ci} is the ratio of carbon content of product i to carbon content of methane molecule and y_{Ci} is the molar fraction of carbon content products in the effluent flow [30]. The molar selectivity was defined as the ratio of

moles of one product and the total moles of products, based on experimental values as shown in previous reports [5 **REF 2015**].

$$X_{Methane}(\%) = \frac{\Sigma\ \gamma_{Ci}\ y_{Ci}}{y_{Methane} + \Sigma\ \gamma_{C\,i}\ y_{C\,i}} \times 100 \qquad (2)$$

2.4 Post reaction analyses

Finally, in order to provide useful information on physicochemical properties of the system, the obtained solid was characterized by XRD and SEM-TEM techniques, allowing the evaluation of the ceramic after catalytic test. For such measurements, the solid was collected after 240 on stream and milled to fine powders.

3. Results and discussion

3.1 Oxide Preparation and Characterization

The chemical composition was calculated by X-ray fluorescence, as shown in Table 1, whose results are close to proposed nominal values, allowing the evaluation of the stoichiometric composition and the correlation between proposed and obtained oxide. The

specific surface area (S_{BET}, m^2 g^{-1}) of pure oxide, displays a high initial surface area in comparison with the same material obtained by means of other techniques [**Reference**].

XRD analysis

The XRD pattern of $LaFeO_3$ oxide after hydrothermal synthesis is shown in Fig. 1. The obtained results indicate the presence of a crystalline structure with the most important reflection signals. By means of a X´pert High Score software it was possible to confirm the presence of the main diffraction signals related to $LaFeO_3$ (JCPDS: 01-088-0641) oxide, in accordance with previous literature [19]. The obtained values of space group, crystal system and cell parameters for the oxide, as shown in Table 2, from which was possible to index a single-phase orthorhombic perovskite structure, without evidence of secondary phases of $La(OH)_3$ or $Fe(OH)_3$ phases was founded. Similarly, Ji *et al.*, has proposed a hydrothermal synthesis route based on the use of glucose in the reaction medium, obtaining good crystallinity levels in short reaction times with subsequent thermal treatments at 650 °C for two hours to aid in the consolidation of crystalline phase. However some problems related with the consolidation of a pure perovskite phase still persist.

TPR analysis

The TPR-H_2 profile of $LaFeO_3$ oxide is shown in Fig. 2. The maximum reduction signal of perovskite occurred under different and progressive signals at 413, 548 and 754 °C, corresponding to the reduction of FeO, Fe_2O_3 and La_2O_3 oxides. According to

Nakamura [20], these results confirm that the solid is reduced in three single steps at different temperatures, kinetically detectable and clearly extended as shown in Eqs 3-6, while solid structure collapses.

$$Fe_2O_3 + H_2 \rightarrow 2FeO + H_2O \quad (3)$$

$$FeO + H_2 \rightarrow Fe^0 + H_2O \quad (4)$$

$$La_2O_3 + 3H_2 \rightarrow 2La^0 + 3H_2O \quad (5)$$

The $LaFeO_3$ samples showed higher intensity peak at higher temperature, which suggests the difficult reduction of La_2O_3, but facilitates the Fe_2O_3 reduction of and consequently the FeO reduction. It suggests that the active sites of the $LaFeO_3$ are localized on Fe ions in coordination with the O_2^- species. These Fe^{3+} ions, located inside the La_2O_3 lattice could not be reduced. Based on obtained XRD results, it cannot be reduced directly to Fe^0 and La_2O_3 respectively. However, the intermediates species containing oxygen deficient structures ($LaFe_xO_{3-y}$) can be reduced until the formation of Fe/La_2O_3.

SEM and TEM analyses

At microscopic level, the synthesized solid is composed by regular crystallites with sizes between 1.0 to 20 μm as shown in Figure 3. These pictures are related to the texture and it is observed the relief formed by the hydrothermal process, favouring a specific morphology in accordance with previous references connected with the hydrothermal

synthesis of rare earth orthoferrites (Zhiqiang Zhou, Li Guo, Haixia Yang, Qiang Liu, Feng Ye. Hydrothermal synthesis and magnetic properties of multiferroic rare-earth orthoferrites. Journal of Alloys and Compounds 583 (2014) 21–31.). Results derived from transmission electron microscopy (TEM) allowed a statistical counting in all micrographs obtained from a population of 100 particles as shown in Fig. 4. The data were recollected and normalized obtaining regular distributions of crystallite sizes with characteristic morphology, confirming previous results derived from X-ray diffraction, where a pure crystalline phase of perovskite oxide was identified. Fig. 5 displays the histogram of the particle size distribution of the obtained powder, showing a unimodal distribution with a marked Gaussian behaviour, which reveals the presence of micrometric particles in the range 1.0 to 20 μm, favoured by the low temperature associated to synthesis process. From transmission electron microscopy data and X-ray diffraction analysis, it was possible to calculate the unit cell of $LaFeO_3$ system, by means of the use of ELMIX software, allowing to find a simulation of the main crystalline parameters from experimental images, as shown in Fig. 6 and Table 2. These results are in agreement with the experimental values obtained by XRD and Rietveld calculations [18].

3.2 Activity and selectivity

The catalytic test was performed at 700 ^{o}C, using a space velocity (GSHV) of 18000 h^{-1}, with a contact time of 0.20 s. The reaction was carried out over a blank and with the oxide sample ($LaFeO_3$) in powder form. Blank results did not show activity. The reaction

was performed after elimination of diffusion or mass transport effects. The conversion H_2/CO ratio and selectivity for H_2 and CO, in all experiments showed an excellent reproducibility. The average methane conversion at 700 ^oC was 66.3 ± 1.08%, and the CO and H_2 selectivity were 96.9 ± 0.99% and 99.1, respectively as shown in Figure 7. The H_2/CO ratio was about 3.0 indicating significant H_2 formation. These results are high compared to the reported values in the literature for different catalysts, while the CH_4 conversion of the Ni/YSZ cermets was of 88% at 900 ^oC [5, 21-23].

The selectivity far from the equilibrium condition and for CH_4 isoconversion was 66% and the CO selectivity was 96% in accordance with Toniolo *et al.* [24]. The XRD and TPR results, showed that the perovskite favours the formation of vacancies and besides, iron at the surface is a stabilizer due to the formation of Fe^{3+}/O^{2-} species at the interface that are the active phase for the CH_4 reforming. In fact, TPR results confirm that $LaFeO_3$ oxide presents oxygen vacancies. According to the literature [25], the methane conversion at 700 °C is quite high due to the strong dependence with bulk oxygen. Lattice oxygen species diffuse from the bulk to surface and increases the reforming reaction [26-28].

Stability

The stability tests were performed during 10 days, using the catalyst under similar reaction conditions. Initially, the sample shows deactivation with time on stream, decreasing progressively 7.1% until 60% methane conversion. After 100 hours with time on stream, the methane conversion and selectivity stabilized. In conclusion, these results

evidenced a high activity, selectivity and stability compared with the Ni supported catalysts or other perovskite oxides such as cobalt, as reported in the literature [29].

3.3 Post-reaction analysis

Scanning and transmission electron micrographs analyses samples post-reaction did not evidence carbon deposition, as shown in Fig. 8. The lanthanum ferrite presents high degree of resistance to carbon deposition after several hours of continuous operation, in accordance with the literature [19]. Moreover, XRD analyses of oxide after testing did not show any structure or composition alteration, discarding the presence of secondary phases, as shown in Fig. 9. Calculations, showed that the space group, crystal and cell parameters, using the ICCD databases, did not show structural modifications. The crystallite size, was calculated using the highest diffraction signals along $D_{(0\ 1\ 1)}$, $D_{(0\ 0\ 2)}$ and $_{(2\ 1\ 1)}$ facets by means of the Debye-Scherrer equation, showing a pronounced increase after catalytic test, including a corresponding loss of the specific surface area, which support the decrease in methane conversion [30, 31].

Although the deactivation of $LaFeO_3$ catalyst is usually attributed to grain sinterization, which depends largely on temperature, time exposure and nature of the reducing environment, among other factors, the catalytic activity decay may result from the promotion of water gas shift reactions (RWGS), mildly exothermic, which occurs rapidly in presence of iron catalysts at temperatures above 400 °C [32] (Eq. 7).

$$CO_2 + H_2 \rightarrow CO + H_2O + \Delta H = 9.0 \text{ kcal/mol} \qquad (7)$$

The steam methane reforming reaction on multicomponent oxides suggests a redox mechanism, where CO reacts with oxygen on active sites forming CO_2. The reduced support is oxidized by water steam, increasing hydrogen concentration and allowing the formation of intermediate species by an associative mechanism. The main reaction occurs between the bidentate intermediate and the terminal hydroxyl groups of the oxide, which is then decomposed to form H_2 and carbonate species [33]. Indeed, the platinum-based catalysts tend to deactivation, due to the high concentration of carbon monoxide. However high concentrations of CO_2, CH_4, or H_2 led to moderate deactivation of oxide. These results suggest that $LaFeO_3$ oxide is a promising ceramic material for eventual application as anodic component in steam methane reforming for development of anodic components in solid oxide fuel cells.

4. Conclusions

The development of one step hydrothermal synthesis method allowed the production of a pure perovskite phase, avoiding the necessity of later stages of calcination. The physicochemical characterization of oxide showed the obtaining of an active and pure phase of $LaFeO_3$ with surface, textural and morphological characteristics related to this wet chemical route. The catalytic test, using the steam methane reforming reaction performed

during 240 hours under isothermal conditions at 700 ºC, showed that methane conversion reach values of 64.7%, with excellent selectivity to carbon monoxide and hydrogen of 97.5 and 99.4 % respectively. The obtaining of by-products, such as CO, CO_2, H_2O, CH_4 and H_2, allows a moderate deactivation of $LaFeO_3$ oxide due to promotion of water gas shift reactions (RWGS), mildly exothermic. Post reaction tests by means of XRD and SEM-TEM analyses, suggests that $LaFeO_3$ oxide is a promising ceramic material for eventual application as anodic component in steam methane reforming for development of anodic components in solid oxide fuel cells.

References

[1] H. L. Chum, R. P. Overend, Fuel Process. Technol. 71 (2001) 187-190.

[2] S. H. Chan, O. L. Ding, Int. J. Hydrogen Energy. 30(2) (2005) 167-179.

[3] R. J. Gorte, J. M. Vohs, J. Catal. 216(1-2) (2003) 477-486.

[4] N. Minh, T. Takahashi, Science and technology of ceramic fuel cells. Elsevier Science, Amsterdam, 1995.

[5] N. F. P Ribeiro, M. V. M. Souza, O. R. Macedo, S. M. R. Vasconcelos, M. Schmal, J. Applied Catalysis A: General. 353 (2009) 305-309.

[6] N. Laosiripojana, S. Assabumrungrat, J. Power Sources. 163 (2007) 943-951.

[7] U. Balachandran, J. T. Dusek, S. M. Sweeney, R. B. Poeppel, R. L. Mieville, P. S. Maiya, M. S. Kleefisch, S. Pei, T. P. Kobylinski, C. A. Udovich, J. Am. Ceram. Soc. Bull. 74 (1995) 71-80.

[8] J. A. Kilner, R. J. Brook, Solid State Ionics. 6 (1982) 237-240.

[9] S. McIntosh, R. J. Gorte, Chem. Rev. 104 (2004) 4845-4865.

[10] S. A. Kramer, H. L. Tuller, Solid State Ionics. 72 (1994) 59-63.

[11] S. J. Xu, W. J. Thomson, Ind. Eng. Chem. Res. 37 (1998) 1290-1295.

[12] M. Alifanti, R. Auer, J. Kirchnerova, F. Thyrion, P. Grange, B. Delmon, Appl. Catal. 41 (2004) 71-74.

[13] K. T. Lee, A. Manthiram, Chem. Mater. 180(6) (2006) 1621-1626.

[14] J. Sfeir, P. A. Buffat, P. Möckli, N. Xanthopoulos, R. Vásquez, H. J. Mathieu, J. Van Herle, K. R. Thampi, J. Catal. 202 (2001) 229-244.

[15] A. L. Dicks, J. Power Sources. 71 (1998) 111-122.

[16] J. Mizusaki, Solid State Ionics. 52 (1992) 79-84.

[17] S. Tao, J. T. S. Irvine, Nat. Mater. 2 (2003) 320-322.

[18] J. A. Gómez-Cuaspud, M. Schmal, Int. J. Hydrogen Energy. 38 (2013) 7458-7468.

[19] D. Bayraktar, F. Clemens, S. Diethelm, T. Graule, J. Van Herle, P. Holtappels, J. Eur. Ceram. Soc. 27 (2007) 2455-2461.

[20] T. Nakamura, G. Petzow, L. J. Gauckler, Mater. Res. Bull. 14 (1979) 649-659.

[21] G. Sierra-Gallego, C. Batiot-Dupeyrat, J. Barrault, F. Mondragón, Rev. Fac. Ing. Univ. Antioquia. 44 (2008) 7-19.

[22] T. Zhang, M. D. Amiridis, Appl. Catal. A: Gen. 167 (1998) 161-172.

[23] R. M De Almeida, H. V. Fajardo, D. Z Mezalira, G. B. Nuernberg, L. K. Noda, L . F. Probst, N. L. V. Carreño, J. Mol. Catal. A: Chem. 259 (2006) 328-335.

[24] F. S. Toniolo, R. N. S. Magalhães, C. A. C. Perez, M. Schmal, Applied Catalysis B: Environmental. 117 (2012) 156–166.

[25] R. J. Gorte, J. M. Vohs, S. McIntosh, Solid State Ionics. 175 (2004) 1-6.

[26] R. Leanza, I. Rosseti, L. Fabbrini, C. Oliva, L. Forni, Appl Catal B. 28 (2000) 55-57.

[27] R. J. Voorhoeve, J. P. Remeika, L. E. Trimble, N. Y. Ann, Acad. Sci, 272 (1976) 3-7.

[28] F. Teng, W. Han, S. H. Liang, B. Gaugeu, R. L. Zong, Y. F. Zhu, J. Catal, 250 (2007) 1-11.

[29] A. M. Silva, L. O. Costa, A. P. M. G. Barandas, L. E. P. Borges, L. V. Mattos, F. B. Noronha, J. Catal Today. 133 (2008) 755-761.

[30] C. H. Bartholomew, Appl. Catal. A: Gen. 212 (2001) 17-60.

[31] P. Forzatti, L. Lietti, Catal. Today. 52 (1999) 165-181.

[32] C. G. Vayenas, S. Bebelis, C. Pliangos, S. Brosda, D. Tsiplakides, Electrochemical activation of catalysis. Kluwer Academic/Plenum Publishers, New York, 2001.

[33] T. Bunluesin, R. J. Gorte, G. W. Graham, Appl. Catal. B: Environ. 14 (1997) 105-l 15.

[34] S. McIntosh, J. M. Vohs, R. J. Gorte, Electrochim. Acta. 47 (2002) 3815-3817.

[35] T. Tsai, S. A. Barnett, J. Electrochem. Soc. 145 (1998) 1696-1699.

Highlights

- Highly pure perovskite oxide of $LaFeO_3$ was obtained from one step hydrothermal synthesis route.
- Catalytic activity of $LaFeO_3$ oxide was tested on steam methane reforming with methane conversions around 66% on dry basis.
- Stability test during 240 hours for steam methane reaction using $LaFeO_3$ oxide, confirms high tolerance to carbon deposition for potential applications.

Caption of tables

Table 1- Elemental composition and surface area of $LaFeO_3$ oxide derived from X-ray fluorescence and BET analysis.

$LaFeO_3$ sample Oxide	**Percent composition**	**Surface area ($m^2 g^{-1}$)**
La_2O_3	67.10 %	67
Fe_2O_3	32.89 %	
Total (100%)	99.99%	

Table 2- Comparison between crystalline properties of perovskite oxide obtained by means of XRD and TEM analysis.

Used technique	**Perovskite oxide**	**Average crystallite size (nm)**	**Space group**	**Crystal system**	**Cell parameters**
XRD	$LaFeO_3$	41.1	*Pbn* (62)	Orthorhombic	*a* = 5,532 Å, *b* = 5,553 Å, *c* = 7,835
TEM	$LaFeO_3$	41.0	*Pbn* (62-63)	Orthorhombic	*a* = 5,425 Å, *b* = 5,453 Å, *c* =

	7,812 Å

Caption of Figures:

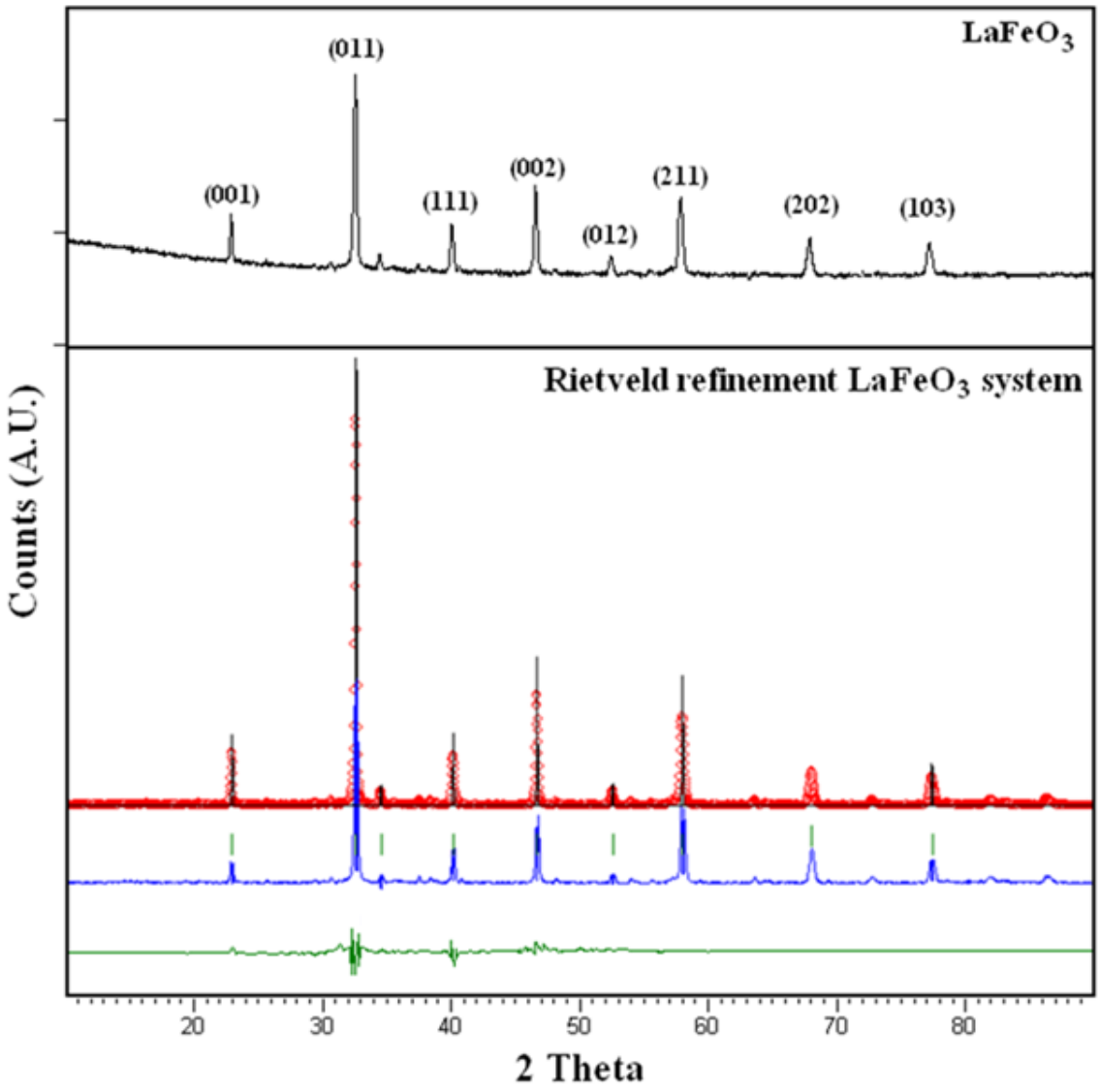

Fig. 1. XRD pattern of $LaFeO_3$ solid obtained by an one step hydrothermal route and compared with corresponding Rietveld refinement.

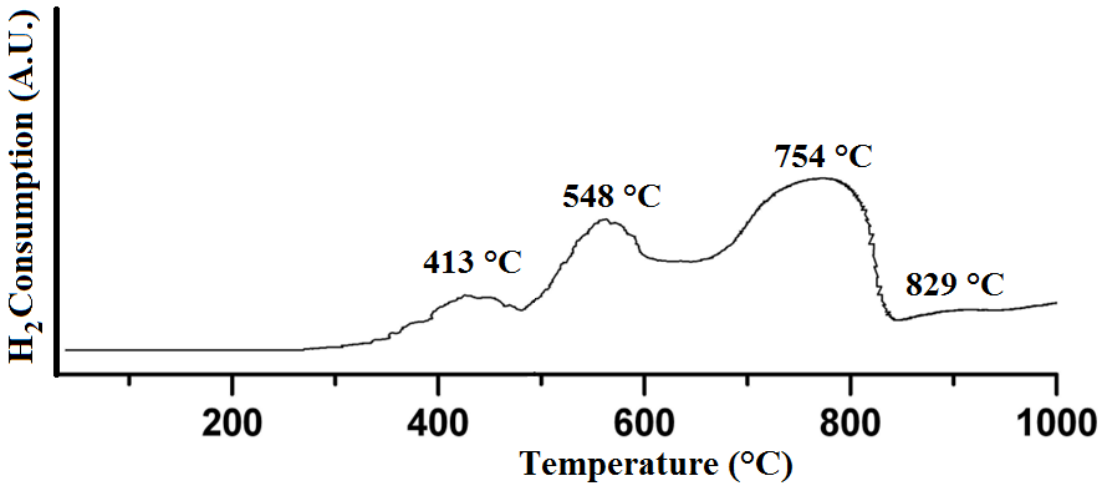

Fig. 2. TPR-H_2 profile for $LaFeO_3$ oxide (10% H_2-He ramping rate 10°C min^{-1}).

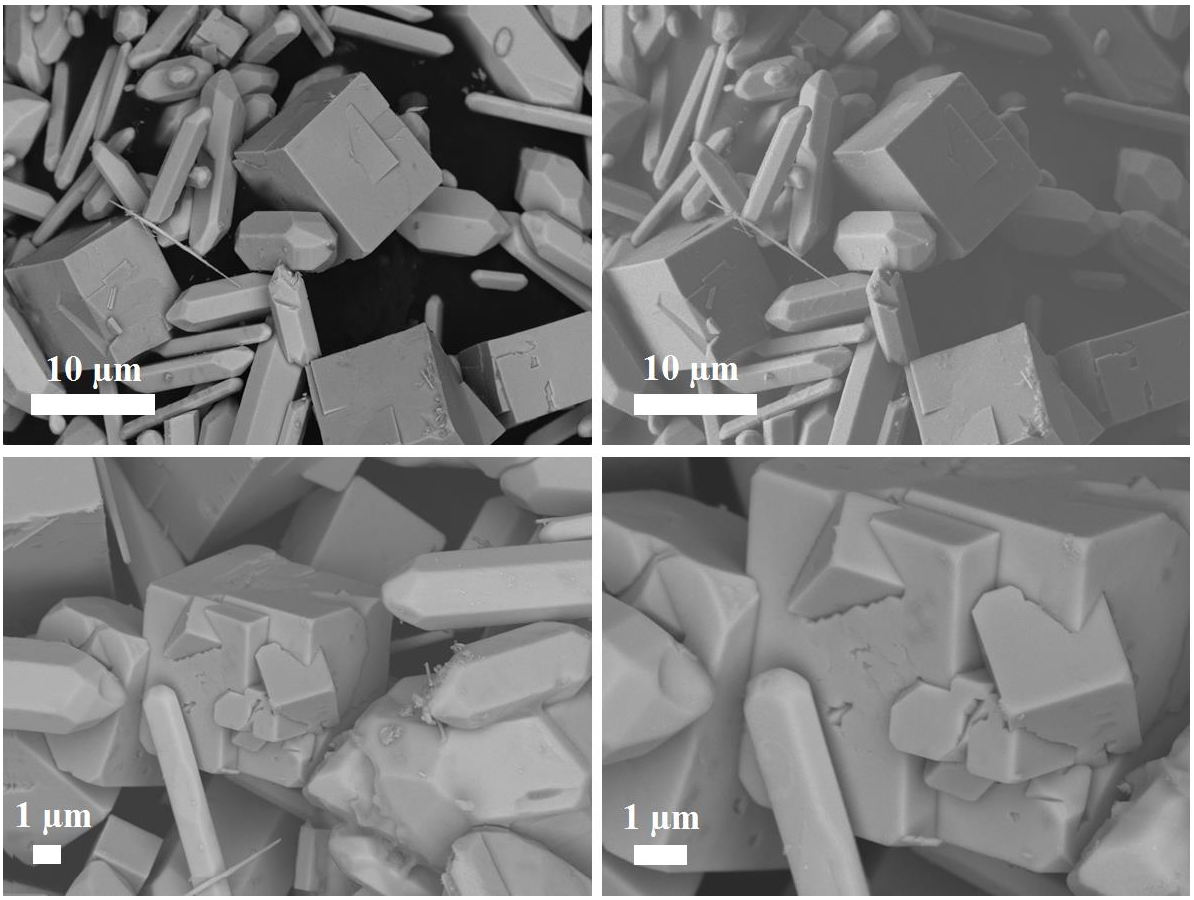

Fig. 3. Micrographs of $LaFeO_3$ solid using secondary and retro dispersed electron microscopy at different magnifications.

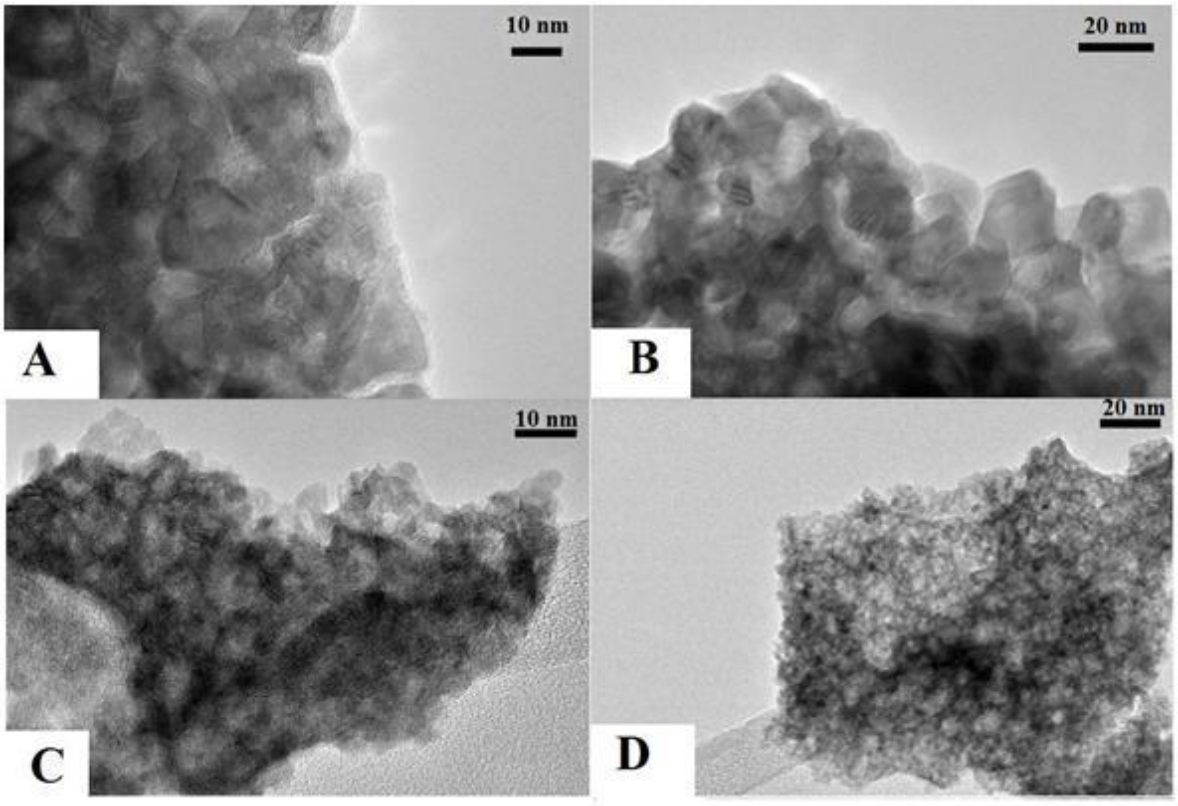

Fig. 4. Transmission electron microscopy micrographs at different magnifications of $LaFeO_3$ solid.

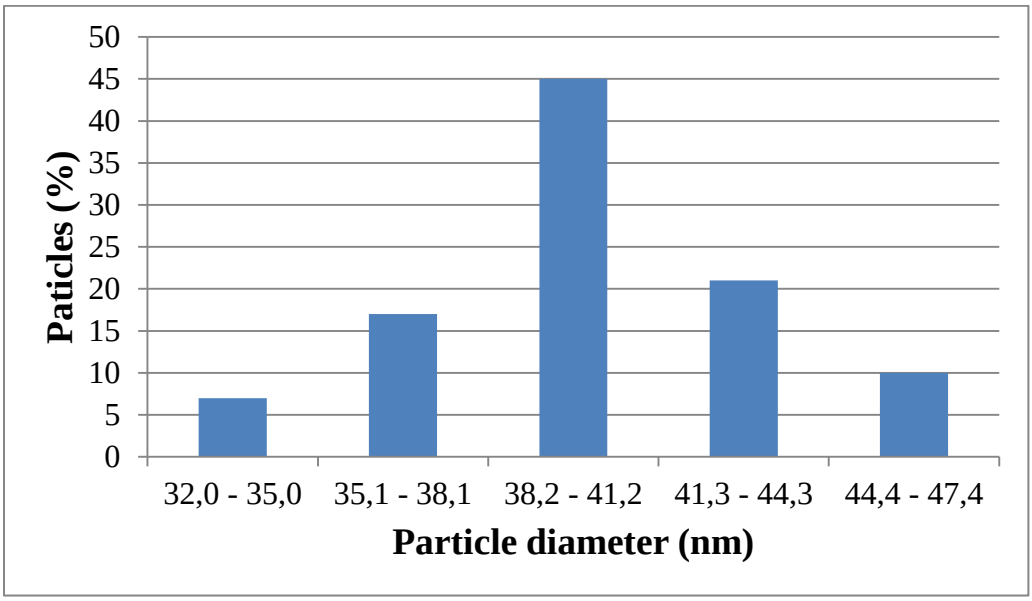

Fig. 5. Histogram distribution of particle size for $LaFeO_3$ sample.

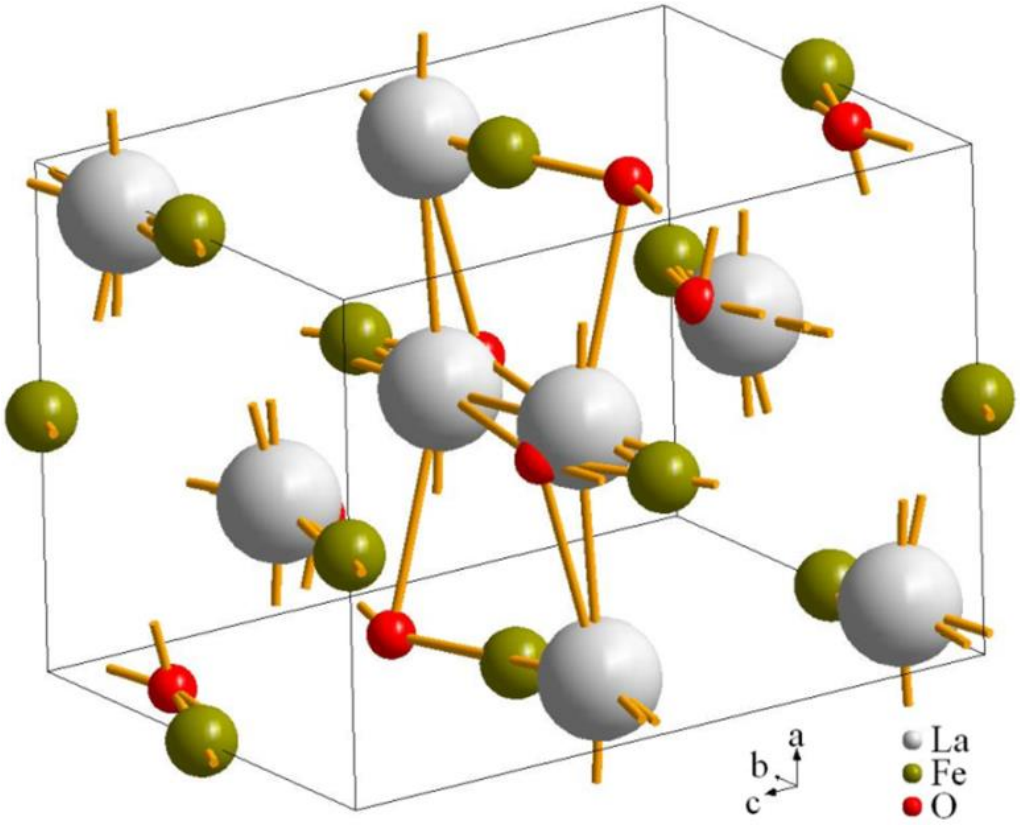

Fig. 6. Unit cell of $LaFeO_3$ system obtained by ELMIX software.

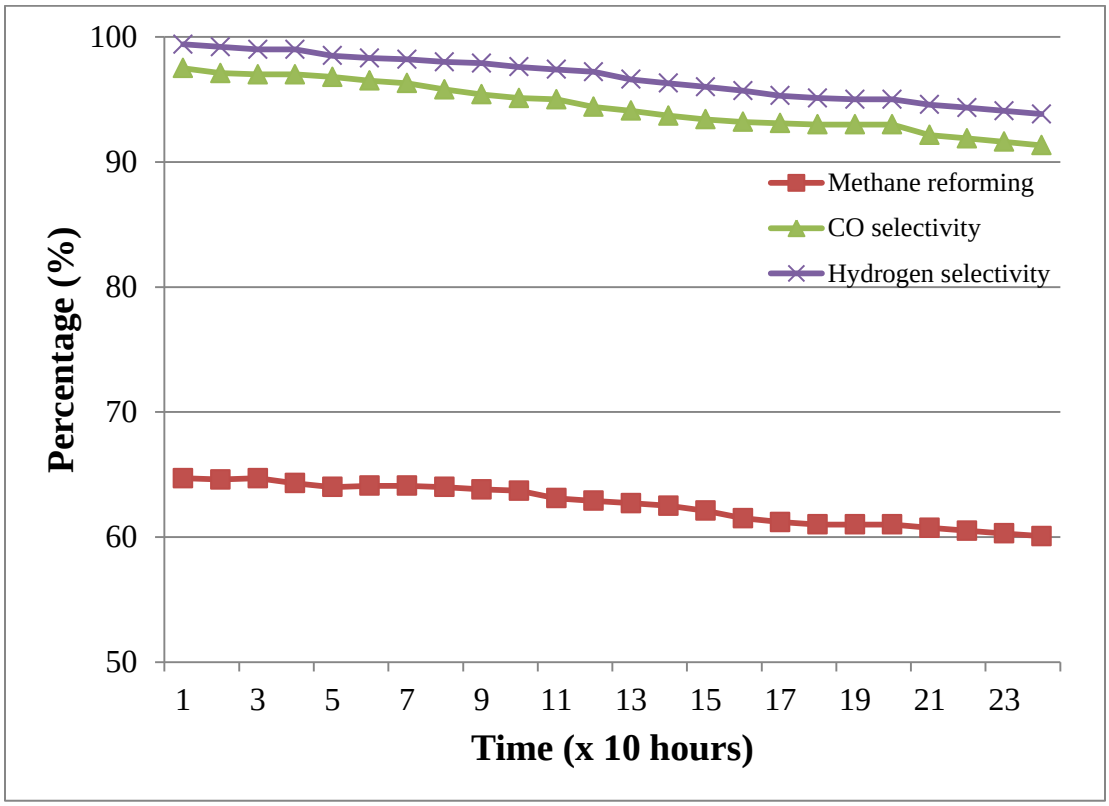

Fig. 7. Stability test during 240 hours for steam methane reaction using $LaFeO_3$ oxide.

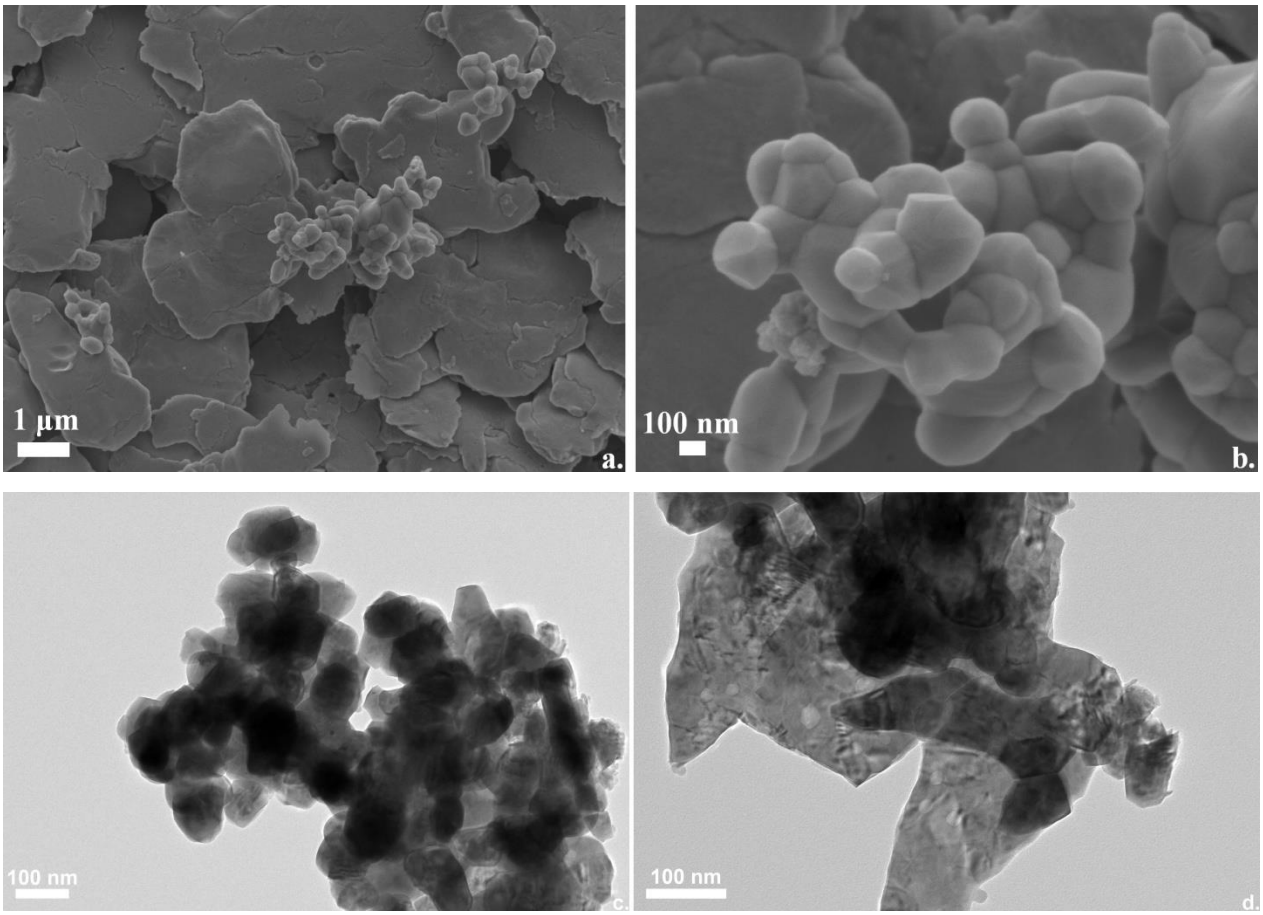

Fig. 8. a. b. SEM and **c. d.** TEM micrographs at different magnifications for $LaFeO_3$ oxide after 240 hours under catalytic test.

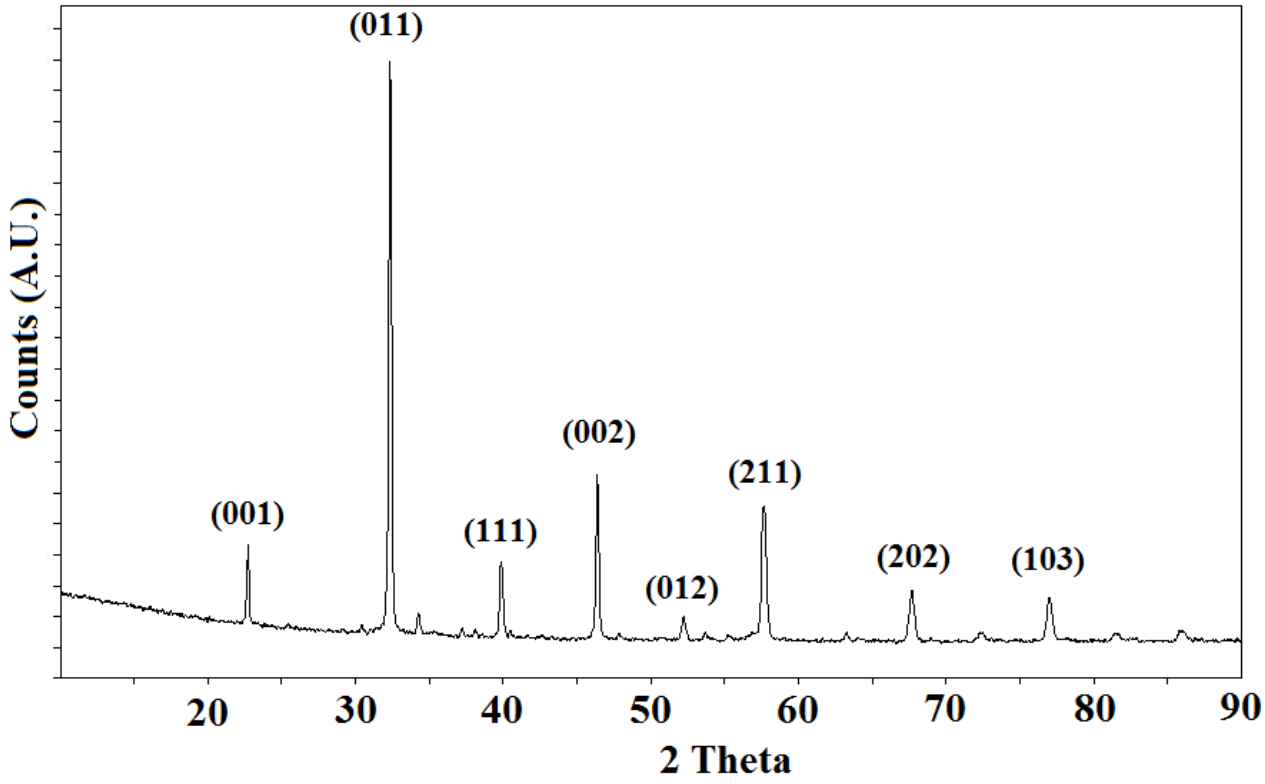

Fig. 9. XRD pattern of $LaFeO_3$ solid after catalytic test during 240 h TOS